Relation of plasma flow structures to particle tracer orbits

L. García[1], B.A. Carreras[2] and I. Llerena[3]

[1]Departamento de Física, Universidad Carlos III de Madrid, 28911 Leganés, Madrid, Spain
[2]BACV Solutions, 110 Mohawk Road, Oak Ridge, Tennessee 37830, USA
[3]Department d'Àlgebra i Geometria, Universitat de Barcelona, 08007 Barcelona, Spain

Corresponding Author: luis.garcia@uc3m.es

Abstract:
Plasma flow structures are analyzed using topological and geometric techniques on the framework of resistive MHD. The structure of the flow is filamentary. The filaments are vortices that are linked to the rational surfaces. The properties of these topological structures are compared with those of tracer particles within a framework of the continuous random walk (CTRW) approach. Vortices may cause some of the trapping of particles, while large scale flows may carry them from vortex to vortex. The results indicate that most of the trappings that are completed during the calculation correspond to tracers trapped on broken filaments, including possible multiple trappings. The probability distribution function of the trapping times is then a function of the filament length, and has a lognormal character, like the distribution of filament lengths

1 Introduction

Turbulence induced transport is one of the outstanding physics problems in plasma physics. In the turbulence induced transport issue, we proceed in three steps. First, the identification of turbulent flow structures using topological and geometric techniques and characterization of their statistical properties [1, 2]. Second, to relate these topological structures to properties of tracer particles within a framework of the CTRW approach [3]. Third, to construct a transport theory based on the CTRW approach and use the information we obtained in characterizing the tracer particle properties. We are working on the framework of the Resistive Magnetohydrodynamic (MHD) turbulence and we are now at the second step in the process.

In the first step of our research, we used topological tools to characterize the flow structures [1, 2]. All the information on the turbulent flow is contained in the electrostatic potential Φ. We define a cubical space covering the cylinder. At a fixed time t, we define a flow structure as the set of points with Φ greater than a given value of the potential. The main finding of Ref. [1] was that the structure of the flow is filamentary. The filaments are vortices that are linked to the rational surfaces. Some of these filamentary vortices close on themselves forming toroidal knots. These are the cycles and they are normally located at the lowest rational surfaces. At the other low rational surfaces the filaments are broken and we characterise them by their length.

The use of particle tracers has proven to be very helpful in trying to understand turbulence-induced transport in magnetically confined plasmas. Particle tracers have been used in numerical simulations to characterize diffusive transport and also non-diffusive transport. Now, we try to use this approach in relating the tracer orbits to flow structures. When we look at tracer particle motion, we see that vortices may cause some of the trapping of particles, while large scale flows may carry them from vortex to vortex. This picture of the particle transport in plasma turbulence is consistent with the interpretation of the transport from the perspective of the CTRW. Here we interpret the tracer trajectories from this point of view.

2 Resistive pressure driven model

In this section, we describe the MHD model equations that we use in calculating the turbulent flows generated by resistive pressure-gradient-driven turbulence that are analyzed in this paper. We study the pressure-gradient-driven turbulence in cylindrical and toroidal geometry by means of a reduced set of resistive MHD equations [4] in the electrostatic limit [5]. For most of the cases considered, the geometry is that of a periodic cylinder, with minor radius a and length $L = 2\pi R$. In this section we describe the equations for the toroidal geometry. The changes when we go to the cylindrical geometry are straightforward.

We use a coordinate system (ρ, θ, ζ), in which ρ is either the normalized minor radius r for the cylindrical case, or a radius-like equilibrium flux surface label for the toroidal case, θ is the poloidal angle and ζ is either the toroidal angle for the toroidal case, or $\zeta = z/R$, where z is the coordinate along the axis of the cylinder, for the cylindrical case. The $E \times B$ velocity is written in terms of the electrostatic potential:

$$\mathbf{V}_\perp = -\frac{\nabla \boldsymbol{\Phi} \times \mathbf{b}}{\mathbf{B}} \tag{1}$$

where Φ is the electrostatic potential, $\mathbf{B}$ is the magnetic field, and $\mathbf{b}$ is a unit vector in the direction of the magnetic field.

The model consists of two equations, the perpendicular momentum equation for the electrostatic potential evolution, and the equation of state for the pressure evolution. The first one is

$$m_i n_i \frac{d\tilde{U}}{dt} = -\mathbf{B} \cdot \nabla \left(\frac{R^2}{\eta F^2} \mathbf{B} \cdot \nabla \tilde{\Phi} \right) + 2 \frac{\mathbf{b} \times \boldsymbol{\kappa}}{B} \cdot \nabla \tilde{p} + m_i n_i \hat{\mu} \nabla_\perp^2 \tilde{U} \tag{2}$$

Here, $d/dt = \partial/\partial t + \mathbf{V}_\perp \cdot \nabla$ is the convective derivative, $U = \boldsymbol{\zeta} \cdot \nabla \times \mathbf{V}_\perp / B$ is the toroidal component of the vorticity, η is the resistivity, $\boldsymbol{\kappa} = \mathbf{b} \cdot \nabla \mathbf{b}$ is the magnetic field curvature, and $\hat{\mu}$ is the viscosity coefficient. The magnetic field is expressed as $\mathbf{B} = F \nabla \zeta + \nabla \zeta \times \nabla \psi$, where $F = RB_\zeta$ is the toroidal flux function and ψ is the poloidal flux. The derivative along the magnetic field can be expressed as

$$\mathbf{B} \cdot \nabla = \frac{F}{R^2} \left(\frac{\partial}{\partial \zeta} - \frac{1}{q} \frac{\partial}{\partial \theta} \right) \tag{3}$$

where q is the safety factor, and R is the major radius. In cylindrical geometry, R and F are constant.

The equation of state for the pressure evolution is

$$\frac{d\tilde{p}}{dt} + \Gamma p \nabla \cdot \mathbf{V}_\perp = D_\perp \nabla_\perp^2 \tilde{p} + D_\parallel \frac{R^2}{F} \mathbf{B} \cdot \nabla \left(\frac{R^2}{F} \mathbf{B} \cdot \nabla \tilde{p} \right) \tag{4}$$

In equations (2) and (4), a tilde identifies perturbed quantities. For the nonlinear calculations, the effect of the $V_\parallel$ evolution in the dynamics of the resistive pressure-gradient-driven turbulence is replaced by a parallel diffusivity in the pressure equation. Viscosity and perpendicular transport are also included in the equations to provide the energy sink needed to get steady-state turbulence.

The driving term of the resistive pressure driven instability is the pressure gradient in the bad curvature region, that is, the second term on the right-hand side (rhs) of equation (2). The first term on the rhs is the field line bending term, which is stabilising. The resistivity weakens this term and allows the instability to grow.

In equation (2), the viscous term of the rhs for the $(m = 0, n = 0)$ component is a viscous drag $-m_i n_i \mu \tilde{U}_{00}$ due to magnetic pumping. In equation (4), an energy source term is added to the rhs for the $(m = 0, n = 0)$ component in order to compensate for dissipation and get a steady state.

The plasma considered here is a model of a configuration of the Large Helical Device (LHD) [6]. Details of the configuration, numerical methods, and main parameters can be found in Ref. [1].

3 Topological analysis of the flow structures

As we have already described in [1], [2], to study the topological structures of the turbulent flow we work with the electrostatic potential Φ. All the information on the turbulence is contained in the function Φ. For instance, turbulence vortices can be easily identified by looking at the contours of the function Φ. We define a cubical space $N_r \times N_\theta \times N_\zeta$ covering the cylinder. At a fixed time t, we define a flow structure as the set of points such that $\Phi(r, \theta, \zeta, t) \geq \Phi_0 \max(\Phi)$, for a suitable constant Φ_0, with $\max(\Phi)$ being the maximum value Φ at time t. Therefore, Φ_0 gives a fraction of the maximum value of Φ and $0 \leq \Phi_0 \leq 1$.

The main finding of Ref. [1] was that, when no average poloidal flow is present, the structure of the flow is filamentary. The filaments are vortices that are linked to the rational surfaces. Some of these filamentary vortices close on themselves forming toroidal knots. These are the cycles and they are normally located at the lowest rational surfaces.

At the other low rational surfaces the filaments are broken and we characterise them by their length. Probably the most remarkable property that we have observed is the lognormal character of the distribution of filament lengths [1]. When an averaged poloidal flow is included in the model, there are also mini-transport barriers created by the shear flow, which were discussed in detail in [2].

4 Relation between flow topology and tracer transport

Having studied the properties of the flow structures, we can now study the statistical properties of the radial displacements of tracer particles during a trapping period when they are moving in the same turbulent flow fields that we have considered in the previous section.

Using the velocity fields obtained from the resistive pressure-gradient-driven turbulence calculations discussed in [1], we have studied the evolution of tracer particles. The velocity field perpendicular to the magnetic field is given in terms of the electrostatic potential, $\Phi(\rho, \theta, \zeta, t)$, by equation (1). Then the evolution of the tracers is given by

$$\frac{d\mathbf{r}}{dt} = -\frac{\nabla\Phi \times \mathbf{b}}{B} + V_0\mathbf{b}, \tag{5}$$

where $\mathbf{r} \equiv (\rho, \theta, \zeta)$ is the tracer position, and V_0 is a constant velocity along the magnetic field lines. In solving this equation we can take Φ at a fixed time and use the frozen field or we can take Φ to be a function of time and then we have a dynamical evolution of tracers. Here, in order to understand better the relation between flow structures and tracer transport, we follow the first option.

When we look at tracer particle motion, we see that vortices may cause some of the trapping of particles, while large scale flows may carry them from vortex to vortex. This picture of the particle transport in plasma turbulence is consistent with the interpretation of the transport from the perspective of the CTRW. Here we interpret the tracer trajectories from this point of view.

First, we decompose the tracer trajectories in radial flights, i.e. radial intervals in between points where the radial velocity changes sign. A sequence of flights around the same radial point corresponds to a trapping; the rest of flights are jumps either between trappings or out of the plasma. These jumps also can have one or many flights. Two examples of a tracer trajectory are shown in figure 1. The tracer on the left panel is trapped during the full length of the calculation, and six different trappings can be identified. The tracer on the right panel is trapped during some time, and then jumps out of the plasma. Precise criteria for trappings are important and far from trivial. Details on the numerical identification of trappings are given in Ref. [7].

For the analysis of the flow structures, we consider 2-D subsets corresponding to $\zeta =$ constant. In each of these toroidal cuts, we identify the connected components following the same approach as we did for the radial slices in [1] and we determine the radial extend of each of them. These connected components are the topological flow structures that

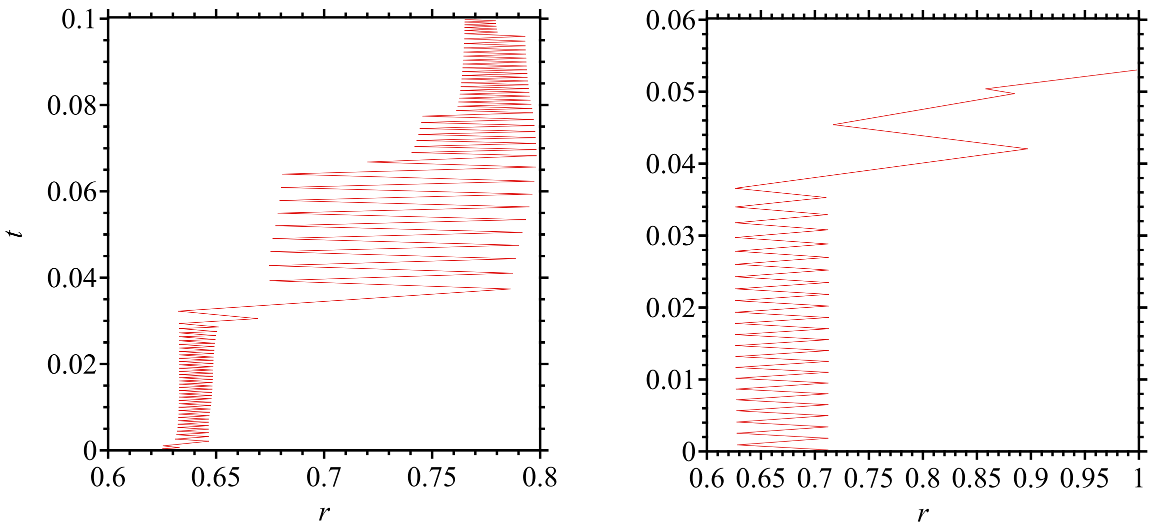

FIG. 1: Examples of tracer trajectories. Left: tracer is trapped during the full length of the calculation. Right: tracer leaves the plasma.

we discuss here. Note that they can be identified with one or more flow vortices. The trapped tracer trajectories are linked to the flow structure not to the individual vortices.

To visualize the topological flow structures and to compare them with the particle tracer orbits, we do first a transformation of the poloidal angle θ to

$$\theta \to \theta + \zeta/q(r) \tag{6}$$

With this transformation, we unscrew the helical structures in such a way that the magnetic field lines became parallel at the axis of the cylinder. Then we can project the structures on the $\zeta = 0$ plane. We can represent this projection in the plane (r, θ); this will give spots that show the maximum width of the structures on the whole ζ range.

Fig. 2 shows the projected structures in the (r, θ)-plane for $\Phi_0 = 0.1$. Also it is shown (in blue) the trajectory of a tracer. The tracer is most of the time trapped at different structures and occasionally jumps between them.

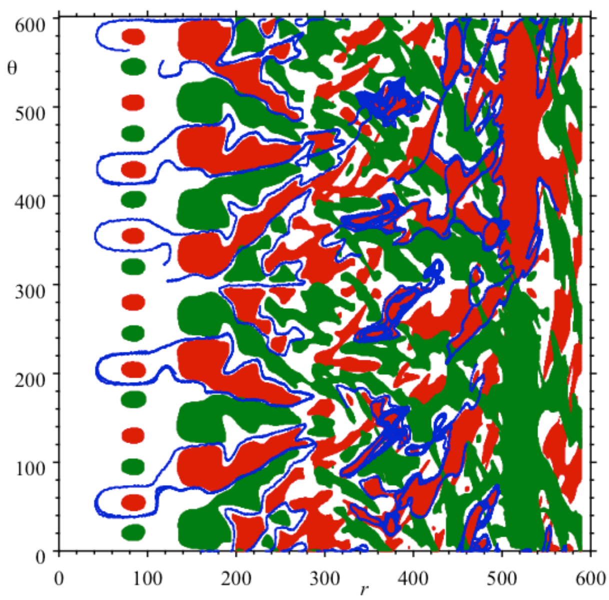

FIG. 2: Projection of flow structures. Points for which $\Phi \geq 0.1\max(\Phi)$ are in red and points for which $\Phi \leq -0.1\max(\Phi)$ are in green. The trajectory of a tracer is shown in blue.

Trappings and flights are closely related to the properties of the plasma flow. Radial excursions are relatively regular during the trapping period but they can vary a great deal from trapping to trapping. Previously, we have found a clear correlation between the radial extend of the flow structures and the radial excursions of the tracer particles during their trapping phase [7]. The character of trapping may change with the magnetic field geometry and by the presence of an averaged flow.

In this paper, we focus on the relation between the trapping times and the flow structures. We have studied the evolution of tracers for three different values of V_0. The initial tracer positions are randomly distributed in the cylinder, and we follow the trajectory of 10^5 tracers till the end of the calculation and accumulate the data. This data is analysed to identify the portion of the trajectories that the tracers remain trapped.

For each case, we have two sets of data on the trapping. There is one set for the trappings that do not reach the end of the calculation, that is, a set of data in which the trapping phase is completed. There is another set in which the tracers were still trapped the last step. In this last set we have tracers that are trapped practically during the full length of the calculation.

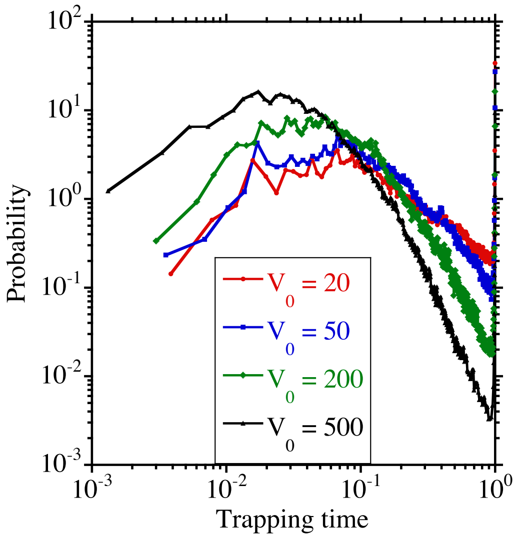

FIG. 3: PDFs of the the trapping times for four values of the parallel velocity.

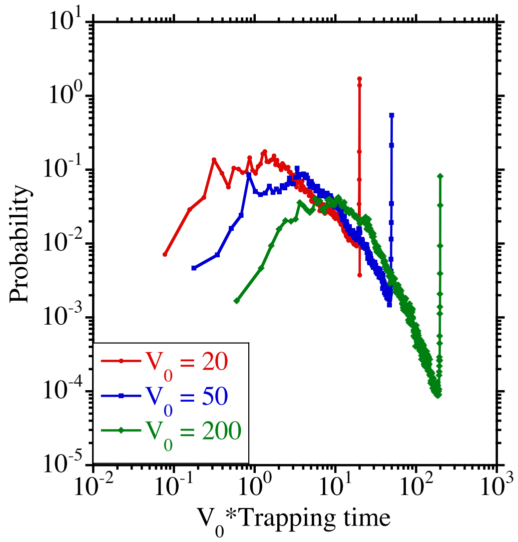

FIG. 4: PDF of the trapping times multiplied by V_0 *for three values of the parallel velocity.*

We have calculated the probability distribution function (PDF) of the trapping times for four values of the parallel velocity of the tracers V_0. The results are shown in figure 3. If we re-scale the trapping times by multiplying by V_0, we have practically the same dependence for the tail of the PDF, as can be seen in figure 4. This indicates that most of the trappings that are completed during the calculation correspond to tracers trapped on broken filaments, including possible multiple trappings (see figure 2). The PDF is then a function of the filament length (product of V_0 by the trapping time). The sharp increase at the end of the distribution corresponds to the tracers which trapping period has not finished by the end of the calculation.

The distribution of trapping times has a lognormal character, like the distribution of filament lengths. This is shown in figure 5, where we plot the PDF of the trapping times for $V_0 = 500$ together with a lognormal fit.

We have developed a model in the line of the CTRW approach for simulating the trapping of tracers.Walks are defined along resonant field lines. For each walk, we take a step δr, which is the radial flight of the tracer when trapped.

For each tracer, the initial radial and poloidal locations are chosen randomly. For the radial step size, δr, we use the distribution of the radial width of the flow structures. For the filaments, the main parameter is the length of the filament along the tracer moves. In this case, we use the lognormal distribution of filament lengths.

The model has two parameters: 1) p_0, the probability that a tracer on a filament jumps to another, and 2) p_1, the probability of a tracer to detrap in a given step.

By choosing suitable parameters p_0 and p_1 we have a reasonable description of the distribution of trapping times and number of flights per trapping.

We have also considered the evolution of tracers in the evolving turbulence, during the same steady state period as we studied the flow structures and using the same turbulent flow field. In general, we have a smoother PDF for the evolving turbulence because of the varying conditions of the flow on one hand and also during the evolution tracers remain trapped for shorter times and the statistics are better than the case of the frozen turbulence. An example of the PDF is shown in figure 6, where it is compared with the PDF for the frozen field case. As shown in Ref. [8], the distribution of trapping times of the tracers is related with the distribution of lifetimes of the cycles in the flow structure.

All the results shown here correspond to turbulence models which do not include an averaged poloidal flow. As we discussed in Ref. [7], when an averaged poloidal flow is self-consistently included in the calculation the trappings are of two types: by vortex structures and by barriers. To distinguish between the two types of trappings we measure the pitch q_p of the averaged tracer trajectory in the (θ, ζ) plane during the trapping. For the tracers trapped in flow structures, this pitch should be equal to $q(r)$, where q is the safety factor at the corresponding radial position. There is an increase in

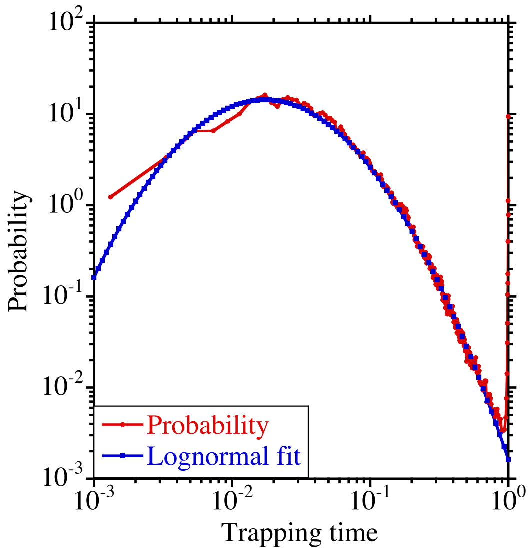

FIG. 5: PDF of trapped times for $V_0 =$ 500 together with a lognormal fit.

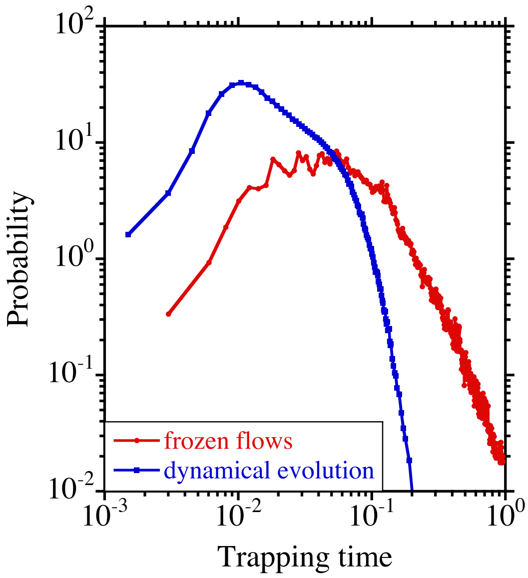

FIG. 6: PDF of trapped times for $V_0 =$ 200 (frozen and evolving field).

the tracer trapping due to tracers trapped in the transport barriers created by the shear in the mean flow.

5 Summary

We have studied the trapping of tracers in a turbulent field in cylindrical geometry. Without an averaged flow, tracers are trapped by vortex-type flow structures and the radial excursions during the trapping correlate well with the widths of these vortex structures.

The trapping of tracers, which do not remain trapped at the end of the calculation, seems to be due to trapping on finite size filaments including multiple possible trappings. The cycles seem to play a role for the tracers that remain trapped very large times, larger than the calculation time.

In the case of tracers in evolving turbulence, the distribution of trapping times of the tracers is related with the distribution of lifetimes of the cycles in the flow structure.

Acknowledgments

This research was sponsored by DGICYT (Dirección General de Investigación Científica y Técnica) of Spain under Project No. ENE2012-38620-C02-02.

References

[1] B. A. Carreras, I. Llerena and L. García, *J. Phys. A: Math. Theor.* **46**, 375501 (2013)

[2] B.A. Carreras, I. Llerena Rodríguez and L. García, *Nucl. Fusion* **54** 103005 (2014)

[3] E. W. Montroll and G. Weiss, *J. Math. Phys.* **6**, 167 (1965)

[4] H.R. Strauss, *Phys. Fluids* **20**, 1354 (1977)

[5] L. Garcia, B.A. Carreras and V.E. Lynch, *Phys. Plasmas* **6**, 107 (1999)

[6] A. Iiyoshi, et al., *Nucl. Fusion* **39**, 1245 (1999)

[7] L. García, I. Llerena Rodríguez and B.A. Carreras, *Nucl. Fusion* **55** 113023 (2015)

[8] B. A. Carreras, L. García and I. Llerena, *Plama Phys. Control. Fusion* **52**, 105005 (2010)